

**ECONOMIC GEOLOGY
RESEARCH UNIT**

University of the Witwatersrand
Johannesburg

**POLYPHASE GRANULITE METAMORPHISM
IN THE VREDEFORT DOME:
A WINDOW INTO THE DEEP KAAPVAAL CRATON
AT 2.06 Ga**

G. STEVENS, R.L. GIBSON and G.T.R. DROOP

INFORMATION CIRCULAR No. 297

UNIVERSITY OF THE WITWATERSRAND
JOHANNESBURG

**POLYPHASE GRANULITE METAMORPHISM IN THE VREDEFORT DOME:
A WINDOW INTO THE DEEP KAAPVAAL CRATON AT 2.06 Ga**

by

G. STEVENS¹, R.L. GIBSON² and G.T.R. DROOP³

(¹ *Economic Geology Research Unit, Department of Geology,
University of the Witwatersrand, P/Bag 3, WITS 2050,
South Africa*

² *Department of Geology, University of the Witwatersrand,
P/Bag 3, WITS 2050, South Africa*

³ *Department of Geology, University of Manchester,
Manchester M13 9PL, United Kingdom)*

**ECONOMIC GEOLOGY RESEARCH UNIT
INFORMATION CIRCULAR No. 297**

February, 1996

POLYPHASE GRANULITE METAMORPHISM IN THE VREDEFORT DOME: A WINDOW INTO THE DEEP KAAPVAAL CRATON AT 2.06 Ga.

ABSTRACT

The numerous greenstone remnants that occur as inclusions in the Archaean gneissic granitoid basement exposed in the core of the Vredefort Dome display evidence of very high grades of granulite facies metamorphism and an unusually complex 3-stage metamorphic history: i) in metapelites, migmatites and refractory restites were produced in a mid-crustal anatetic event, at temperatures in excess of 900 °C (in the restites) (M_1); ii) in the migmatites, the peak metamorphic assemblages are variably overprinted by a high-grade retrograde reaction that involved crystallizing anatetic melts (M_2); iii) both the peak metamorphic assemblages and the retrogression textures are cross cut by pseudotachylite breccia veins that mark a shock metamorphic event associated with the formation of the Vredefort Dome; and, iv) the peak metamorphic assemblages and the retrogression textures are overprinted by new generations of remarkably fine-grained, post-shock, high-grade phases that crystallised at a pressure some 0.25 GPa lower than that of both the peak metamorphic conditions and the retrogression (M_3). These data indicate an anticlockwise P - T evolution where mid-crustal anatexis resulted from the intraplating of Bushveld Complex-related ultramafic magmas at 2.06 Ga. A period of approximately isobaric cooling and retrogression was followed by the Vredefort Catastrophe that resulted from the impact of a large meteorite into the terrane at 2.02 Ga. This shock event halted the natural mid-crustal metamorphic progression prior to the terrane cooling below 650°C, and resulted in the rapid exhumation of the terrane by some 9 km. In the process it has provided a window into the deep levels of the central Kaapvaal Craton not seen elsewhere in the region.

oOo

**POLYPHASE GRANULITE METAMORPHISM IN THE VREDEFORT DOME:
A WINDOW INTO THE DEEP KAAPVAAL CRATON AT 2.06 Ga.**

CONTENTS

| | Page |
|---|-------------|
| INTRODUCTION | 1 |
| GEOLOGICAL SETTING | 3 |
| PRE-SHOCK METAMORPHISM | 6 |
| M₁, peak metamorphism | 6 |
| P-T conditions during M₁ | 9 |
| Prograde conditions | 10 |
| Cooling from the metamorphic peak | 11 |
| M₃, POST-SHOCK METAMORPHISM | 11 |
| ORIGIN OF THE METAMORPHISM | 16 |
| CONCLUSIONS | 18 |
| ACKNOWLEDGEMENTS | 19 |
| REFERENCES | 19 |
| APPENDIX | 24 |

_____oOo_____

**Published by the Economic Geology Research Unit
Department of Geology
University of the Witwatersrand
1 Jan Smuts Avenue
Johannesburg 2001
South Africa**

ISBN 1 86838 196 X

POLYPHASE GRANULITE METAMORPHISM IN THE VREDEFORT DOME: A WINDOW INTO THE DEEP KAAPVAAL CRATON AT 2.06 Ga.

INTRODUCTION

The development of regional-scale granulite facies metamorphism at depths corresponding to mid-crustal levels in continental crust requires an extreme perturbation of the thermal structure of the crust by tectonic and/or magmatic processes (e.g. Harley, 1989 and references therein). In general, such extreme perturbations require an intensity of tectonic activity that is most likely to be found along the established or incipient margins of continental plates where processes such as rifting, plate convergence and subduction disturb the steady-state thermal structure of the crust. Along these active plate margins, rocks that record details of the consequent metamorphic episode commonly become exposed at surface. This has resulted in a relatively good understanding of the thermal and baric evolution of the crust in these environments. The nature of mid- to lower-crustal metamorphism associated with magmatism within cratonic environments is more enigmatic. Such magmatism points to transient thermal perturbations in the lithosphere and asthenosphere underlying crust that may not have experienced significant exhumation for hundreds and even thousands of millions of years. Consequently, our knowledge of the thermal evolution of the deep cratonic crust during anorogenic magmatism is limited. In most cases it is restricted to information gained from studies of xenoliths of deep crustal material sampled during younger extrusive events.

The Kaapvaal Craton of southern Africa represents one of the oldest known cratonic fragments. Geochronological studies indicate that sialic crustal fragments were present as early as 3.7 Ga and the bulk of the craton had accreted by ~3.0 Ga (De Wit *et al.*, 1992). Since this time only limited exhumation has occurred, resulting in the preservation of Archaean and early Paleoproterozoic sedimentary basins over much of the craton (Fig. 1). The craton experienced a major magmatic event some 1000 Ma after consolidation. The 2.05-2.06 Ga (Walraven *et al.*, 1990; Walraven and Hattingh, 1993) Bushveld magmatic event led to the extrusion of voluminous felsitic volcanics of the Rooiberg Group, and concomitant intrusion of up to 6 km of mafic-ultramafic magmas and younger granites of the Bushveld Complex into the upper levels of the Proterozoic Transvaal Supergroup (Fig. 1). The presence of the crustally derived felsitic lavas (Hatton and Schweitzer, 1996) and late-stage granites associated with the Complex indicate an extreme thermal perturbation of the deep cratonic crust and large-scale crustal anatexis. This suggests that deep crustal levels in the Kaapvaal Craton that were subjected to this event should record evidence of a ca. 2.05-2.06 Ga regional, ultra-high temperature metamorphic event. To date, no high-grade metamorphic rocks on the Kaapvaal Craton have been correlated with this event, largely due to a lack of exposure of deep crustal levels. However, sapphirine-bearing granulites, equilibrated at >900 °C and 0.7 to 1.0 GPa (Dawson and Smith, 1987), that occur as xenoliths in the Lace Kimberlite (Fig. 1) possibly hint at the existence of a high-grade terrane underlying the central Kaapvaal Craton. In one area, however, deep crustal rocks are exposed - the Vredefort Dome (Fig. 1), located some 120 km south-southwest of Johannesburg, is a mid-Proterozoic domal structure that exposes within its core Archaean basement rocks that contain

evidence of high-grade metamorphism. In this paper it is proposed that the formation of the Vredefort Dome led to the fortuitous sampling of hot cratonic basement cooling after a thermal peak induced by Bushveld magmatic activity. This provides a unique insight into the metamorphic evolution of an undiscovered mid-crustal regional granulite terrane that probably underlies a significant portion of the central Kaapvaal Craton.

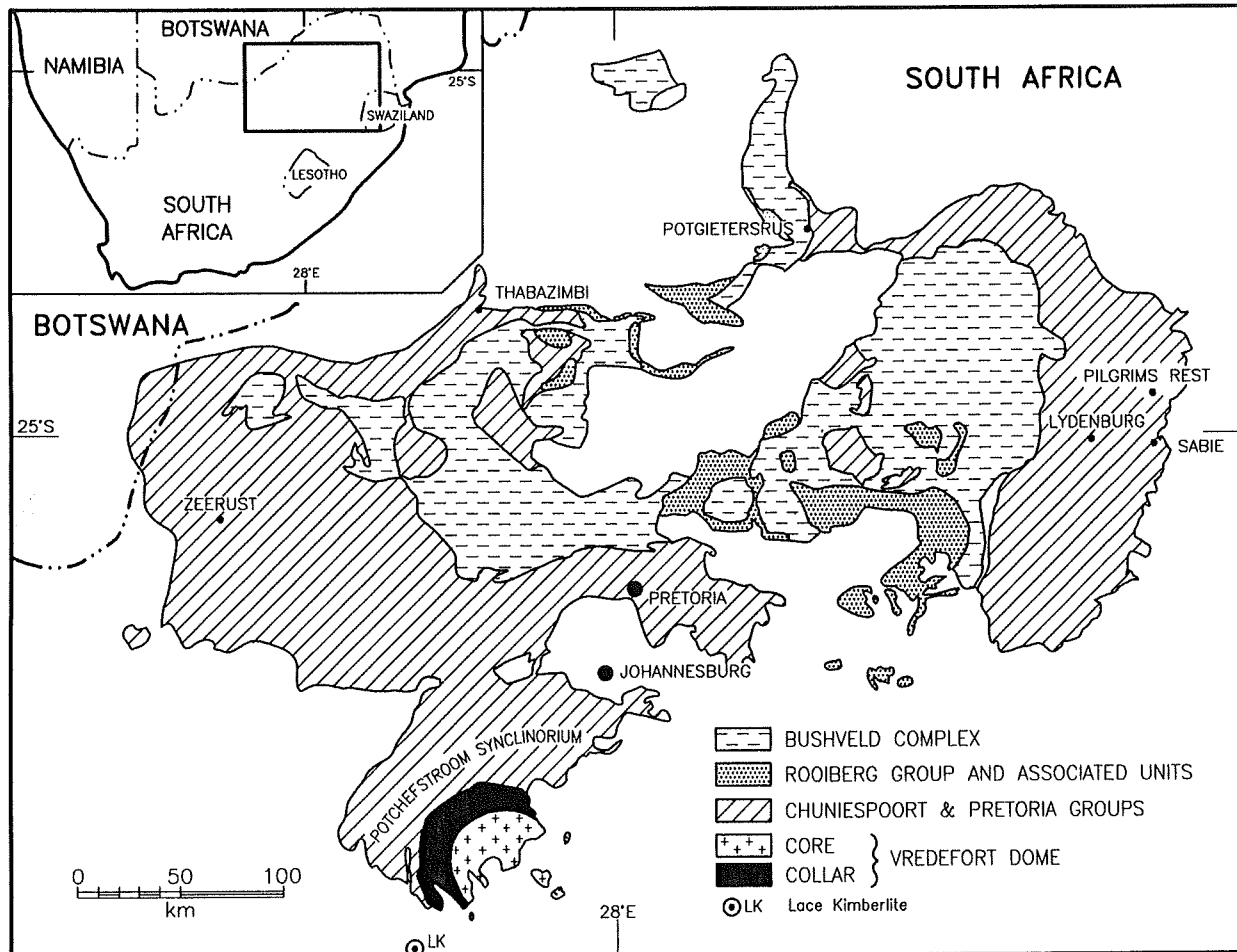


Figure 1: The geographic position of the Vredefort Dome relative to the present day exposures of mafic-to-ultramafic intrusives of the Rustenburg Layered Suite of the Bushveld Complex and the rhyolitic extrusives of the Rooiberg Group. The present day outcrop limits of portions of the Chuniespoort and Pretoria Groups of the Transvaal Supergroup are also indicated. Note that erosional remnants of the Rooiberg Group occur within 150 km of the Vredefort Dome. The position of the Lace Kimberlite is also illustrated.

GEOLOGICAL SETTING

The Vredefort Dome is an ~80 km wide structure that forms a structural and thermal "high" within the Witwatersrand Basin. The ~45 km diameter core of the Dome comprises > 3.1 Ga gneissic, granitoid basement, with subsidiary rafts of supracrustals (metapelites, metagreywackes and meta-iron formation) and dismembered mafic intrusions of greenstone affinity (Stepto, 1990). The core is surrounded by a 15-20 km wide collar of generally subvertically dipping supracrustal rocks belonging to the Dominion Group and the Witwatersrand, Ventersdorp and Transvaal Supergroups (Fig. 2) which range in age from ~ 3.0 to ~2.2 Ga. The collar rocks contain numerous mafic sills and dykes, most of which appear to be related to the Ventersdorp and Bushveld Complex events (Bisschoff, 1972). Several small peralkaline and dioritic igneous complexes also occur, and are believed to be older than the Bushveld Complex (ca. 2.2 Ga, Walraven and Elsenbroek, 1991). The Dome is unconformably overlain in the south by Phanerozoic sediments and intrusions of the Karoo Supergroup.

The formation of the Vredefort Dome was accompanied by widespread regional deformation. The 35 km-wide rim synclinorium surrounding the Dome is believed to be largely responsible for the preservation of the remnants of the Witwatersrand Basin (McCarthy *et al.*, 1990) and deformation structures attributed to the doming event (folds, cleavages, thrusts) have been identified up to 150 km from the Dome (McCarthy *et al.*, 1986). In addition, the rocks in the Dome contain abundant evidence of shock deformation (shatter cones, planar microdeformation features, coesite and stishovite, voluminous pseudotachylites) which has been construed as evidence in support of a meteorite impact origin for the Vredefort Dome (see Reimold, 1993 for a comprehensive review). Calculations by Grieve *et al.* (1981) and Therriault *et al.* (1993) suggested that the original diameter of the impact structure, of which the Vredefort Dome forms the central uplift, was between 180 and 300 km, covering most of the Witwatersrand Basin. The ca. 2.0 Ga age of the doming event was originally constrained from radiometric studies of granophyre dykes (2016 ± 24 Ma (K-Ar isochron from biotite) and 2002 ± 52 Ma (U-Pb zircon) (Walraven *et al.*, 1990), 2006 ± 9 Ma (biotite Ar-Ar, Allsopp *et al.*, 1991)) believed to represent remnants of an impact melt sheet (French and Nielsen, 1990). These results are in close agreement with recently obtained ages of 2006 ± 17 Ma (Ar-Ar stepheating, Trieloff *et al.*, 1994), 2018 ± 7 Ma (weighted mean, Ar-Ar laser probe, Spray *et al.*, 1995) and 2024 Ma (U-Pb zircon, Kamo *et al.*, 1995) from pseudotachylite veinlets, which are also believed to be a consequence of the impact event.

The metamorphic grade of rocks exposed in the Vredefort Dome increases radially inwards (Fig. 3). The transition from greenschist facies grades, developed in the outer parts of the collar, to amphibolite facies grades occurs in the lower parts of the Witwatersrand Supergroup (mid-Government Subgroup). The rocks in the outer parts of the basement core, comprising granitic

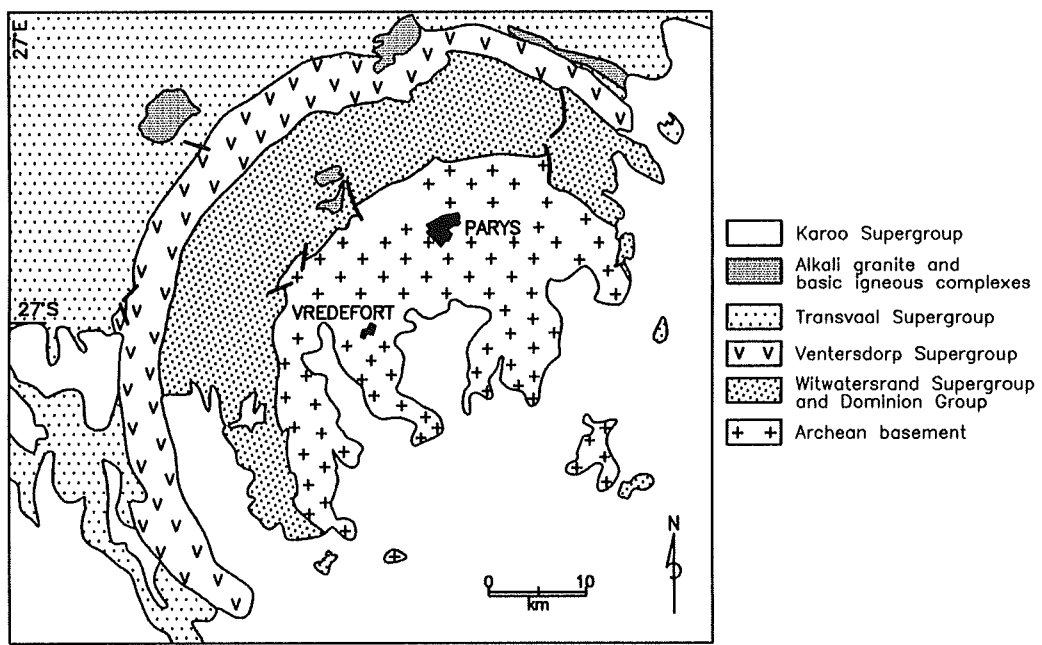


Figure 2: Simplified geological map of the Vredefort Dome.

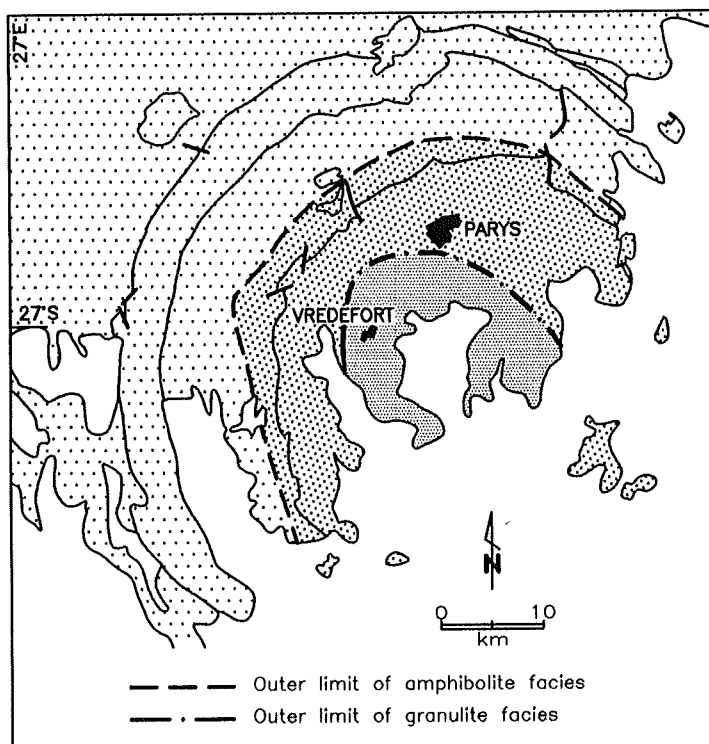


Figure 3: The distribution of metamorphic facies in the Vredefort Dome (modified from Gibson and Wallmach, 1995). All the samples described in the present study are from the granulite core.

-to-granodioritic migmatitic gneisses (the Outer Granite Gneiss, Stepto, 1990) contain upper amphibolite facies assemblages (Nel, 1927; Bisschoff, 1982), whereas those in the centre of the Dome, comprising leucogranulites and subsidiary paragneisses and mafic orthogneisses (Inlandsee Leucogranofels Terrane and Steynskraal Formation, Stepto, 1990) contain granulite facies assemblages (e.g. Schreyer and Abraham, 1978; Schreyer *et al.*, 1978; Stepto, 1990). The amphibolite-granulite transition occurs approximately 8-10 km from the core-collar contact (Fig. 3) (Bisschoff, 1982; Stepto, 1990).

The metamorphic history of the rocks in both the collar and the core has historically been very poorly constrained. However, recent advances have been made in a study of the amphibolite facies lower Witwatersrand metapelites in the collar (Gibson and Wallmach, 1995) indicating a complex, two-stage metamorphic history. An anticlockwise P - T loop has been described (Fig. 4), with the peak of metamorphism (M_{1a} of Gibson and Wallmach, 1995) occurring prior to pseudotachylite formation as evidenced by pseudotachylite veins truncating the peak amphibolite facies assemblage. Pseudotachylite formation is inferred to have occurred under lower amphibolite facies conditions, at slightly lower temperatures than the peak of metamorphism, as the veins are recrystallised to lower amphibolite grade assemblages (M_{1b} of Gibson and Wallmach, 1995). Petrogenetic modelling in the simplified KFMASH system by Gibson and Wallmach (1995) indicated that the M_{1b} assemblage crystallised at a pressure at least 0.1 to 0.15 GPa lower than that of the M_{1a} assemblage. Thus, shock metamorphism in the collar, as marked by pseudotachylite formation, coincided with a period of decompression.

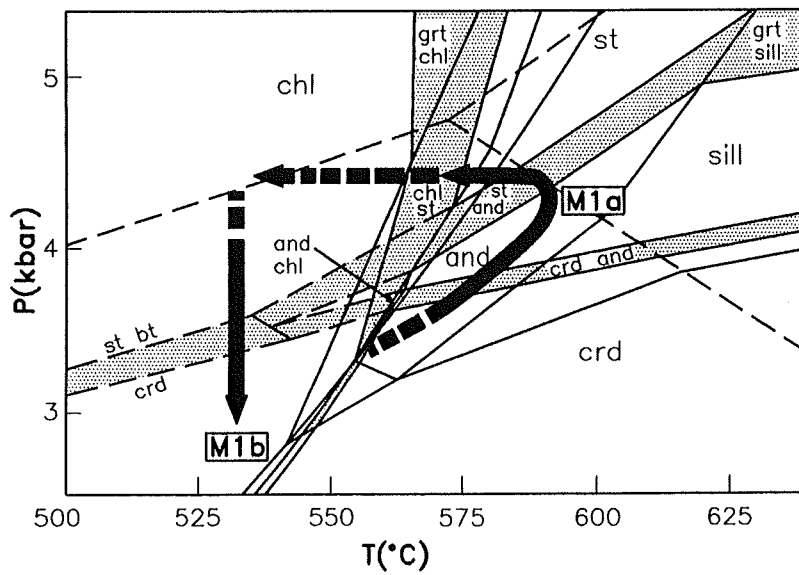


Figure 4: The P-T path proposed for the amphibolite grade rocks of the collar by Gibson and Wallmach (1995). The anticlockwise loop is characterised by peak M_{1a} assemblages that are truncated by pseudotachylite breccias and a related brittle cleavage. These phenomena are overprinted by lower-pressure M_{1b} cordierite + biotite assemblages.

The metamorphic history of the core granulites has remained largely unconstrained although the limited work that has been done suggests a complex history with the possibility of several events (e.g. Stepto, 1990). Hart (1978) proposed an extensive granulite facies event at 3.5 Ga. Further geochronological studies suggested that the basement was affected by events at approximately 3.1 and 2.8 Ga (e.g. Hart et al., 1981; Allsopp et al., 1991). A fourth event is thought to be intimately associated with the formation of the Dome at ~2.0 Ga (e.g. Schreyer, 1983; Stepto, 1990). Stepto (1990) was, however, equivocal about the exact timing, claiming that the metamorphic peak was either pre- or syn- uplift of the Dome (p. 101) or that it was post-doming (p. 93). Interpretation of the metamorphism in the core is further complicated by evidence that shock-related phenomena (e.g. pseudotachylite), believed to be the result of the ca 2.0 Ga impact, postdate some high-grade metamorphic assemblages, yet predate other high-grade mineral associations (e.g. Schreyer and Abram, 1978; Schreyer, 1983). Thus, as in the collar, pre- and post-shock metamorphic assemblages can be defined on the basis of their relationship to pseudotachylite. This has been perceived by some workers as evidence in favour of a localised igneous heat source below the Dome and an endogenic process of dome formation (e.g. Schreyer and Abram, 1978; Schreyer, 1983). The post-shock metamorphic features clearly indicate that the basement beneath the Dome was at elevated temperature after the dome-forming event (Grieve et al., 1990; Martini, 1992), as does the 1944 ± 92 Ma Rb-Sr whole-rock age obtained for a small granitoid body (the Central Anatetic Granite of Hart et al. (1981)) in the core of the Dome that is believed to be of local anatetic origin. This study builds on this polymetamorphic model, but seeks to clarify the relationship of the pre- and post-shock metamorphism to dome formation and to identify the driving mechanisms behind both metamorphic events by quantifying the *P-T* evolution of the metasedimentary granulites in the core.

PRE-SHOCK METAMORPHISM

The pre-shock metamorphic textures are characterised by well-equilibrated coarse-crystalline assemblages that clearly predate the pseudotachylite-forming event. These early textures are invariably overprinted by later events, but sufficient useful data has been gained to allow the early metamorphic evolution to be constrained.

M₁, peak metamorphism

Migmatisation features represent the earliest discernable metamorphic textures in most of the metasedimentary granulites exposed in the core. In many of these exposures there is convincing field evidence for anatetic processes. Several authors have described the local formation of anatetic melts in the Vredefort core (e.g. Bisschoff, 1982; Schreyer, 1983), but no detailed studies of the anatetic features was attempted. Field evidence at locality VG3 on the farm Steynskraal is typical of many of the metapelitic exposures examined in this study. Large garnet and cordierite crystals have been produced in conjunction with stromatic leucosomes of quartz,

plagioclase and K-feldspar that are parallel to a relic foliation or compositional layering (Fig.5) giving rise to coarsely crystalline garnet-cordierite migmatites. The same event in less aluminous metagreywackes produced similar garnet-cordierite-orthopyroxene migmatites. The growth of coarse crystals of garnet, with or without cordierite and/or orthopyroxene, in association with leucosome development, has been described from many anatetic terranes (e.g. Powell and Downes, 1990; Stevens and Van Reenen, 1992; Srogi *et al.*, 1993). Such evidence indicates incongruent melting involving biotite breakdown to produce an H₂O-undersaturated granitic melt and a mafitised, residual, crystalline assemblage (e.g., in metapelites, Bt + Sil + Qtz + Pl = Melt + Grt + Crd ± Kfs). Reactions of this type are always multi-variant in chemically complex natural systems and biotite-bearing migmatised exposures represent rocks that equilibrated at *P-T* conditions within the melting reaction field, or where the consumption of a reactant phase, other than biotite, halted the reaction.

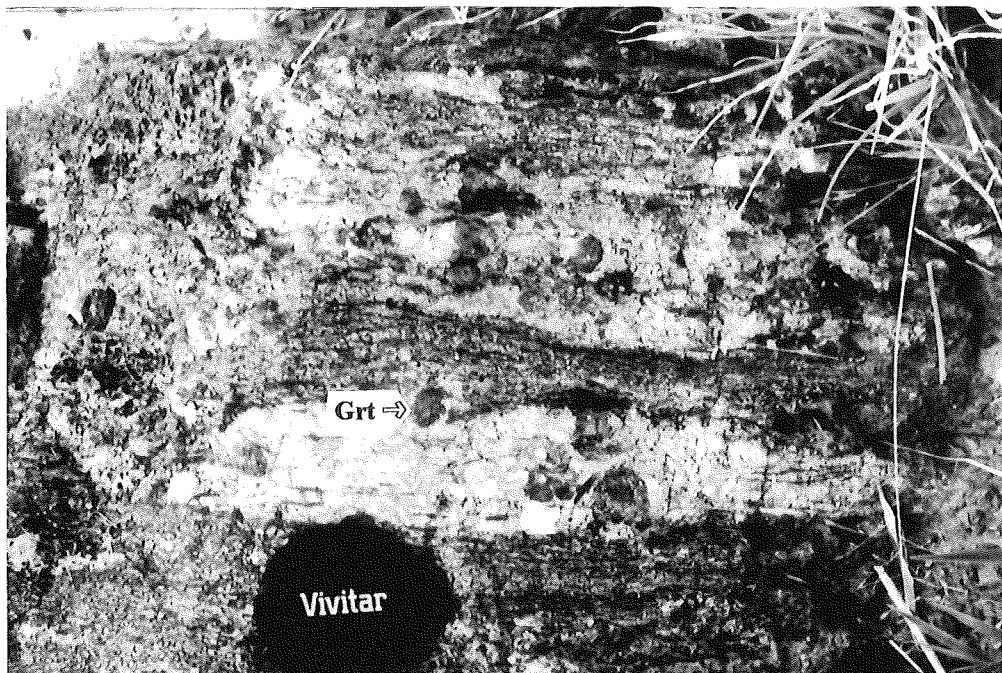


Figure 5: Typical anatetic field relations at the locality VG3. Note the large garnet (Grt) crystals developed in conjunction with the granitic leucosomes.

In other exposures, metasediments (Table 1) are not migmatised. Rather, they have the mineralogical and chemical composition of melt-depleted restites. In such samples the temperature of peak metamorphism exceeded the maximum for biotite - H₂O-undersaturated melt coexistence and the bulk of the melt (and the H₂O component dissolved within it) was mobilized out of the system. This process has produced metasedimentary restites that can be subdivided into garnet-quartz, garnet-cordierite, and cordierite restites, reflecting a bulk rock compositional control on the mineralogy of the restitic products of the biotite incongruent melting reaction (Fig. 6).

Table 1: Bulk rock compositions for the metasedimentary granulites examined in this study. All Fe is expressed as Fe₂O₃. (a) cordierite restites; (b) garnet-quartz restite; (c) garnet-orthopyroxene restites; (d) migmatites

| | (a) | (b) | (c) | | | (d) | | | | |
|------------------------------------|--------|--------|-------|-------|-------|-------|-------|--------|--------|-------|
| | V486 | V624 | V600 | V206 | V466 | V700 | VGS3 | VGS4 | V595 | V405 |
| SiO₂ | 55.63 | 54.50 | 58.49 | 54.56 | 63.91 | 60.67 | 58.23 | 63.25 | 63.53 | 59.77 |
| TiO₂ | 0.27 | 0.31 | 0.28 | 0.27 | 0.28 | 0.31 | 0.28 | 0.31 | 0.42 | 0.29 |
| Al₂O₃ | 27.11 | 25.47 | 16.56 | 13.50 | 13.64 | 14.41 | 18.23 | 18.36 | 18.31 | 16.97 |
| Fe₂O₃ | 4.78 | 10.38 | 14.74 | 23.32 | 11.68 | 11.98 | 10.67 | 7.08 | 6.99 | 10.25 |
| MnO | 0.06 | 0.15 | 0.42 | 0.46 | 0.20 | 1.50 | 0.25 | 0.11 | 0.07 | 0.15 |
| MgO | 1.78 | 1.87 | 2.90 | 5.49 | 4.59 | 4.64 | 5.03 | 4.96 | 5.23 | 6.57 |
| CaO | 1.42 | 0.20 | 2.84 | 1.42 | 1.11 | 1.44 | 1.48 | 1.24 | 0.94 | 0.55 |
| Na₂O | 2.58 | 2.46 | 2.49 | 0.26 | 1.83 | 1.86 | 2.23 | 1.92 | 1.46 | 1.08 |
| K₂O | 5.44 | 3.54 | 0.59 | 0.31 | 1.23 | 1.54 | 2.31 | 2.38 | 3.74 | 2.94 |
| P₂O₅ | 0.06 | 0.05 | 0.25 | 0.35 | 0.04 | 0.06 | 0.09 | 0.06 | 0.11 | 0.04 |
| LOI | 1.16 | 1.69 | 0.00 | 0.02 | 0.01 | 0.54 | 0.73 | 1.03 | 0.60 | 0.34 |
| Total | 100.26 | 100.62 | 99.39 | 99.93 | 98.52 | 98.94 | 99.51 | 100.69 | 101.40 | 98.95 |

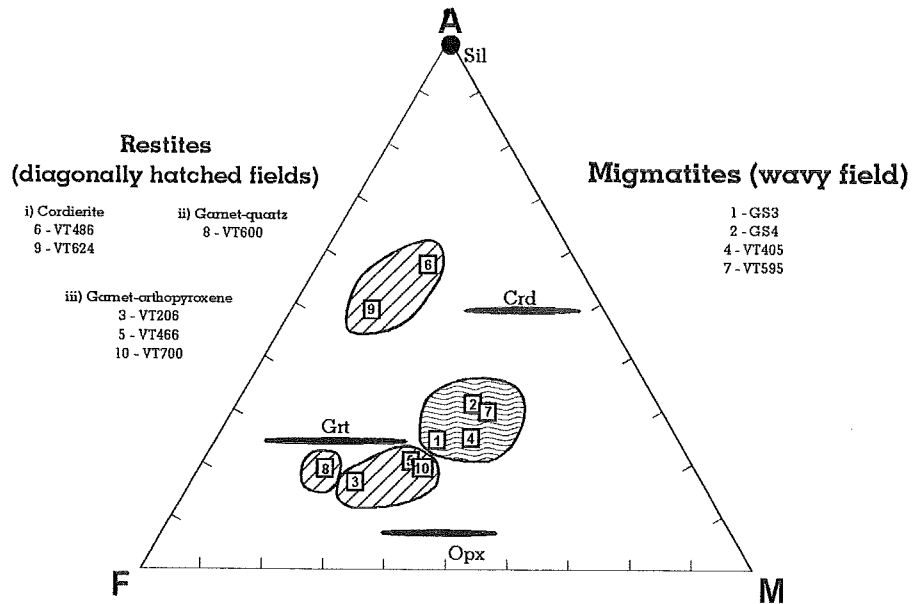


Figure 6: AFM projection from quartz, plagioclase and K-feldspar for the metamorphic assemblages in the different bulk composition groups. This plot assumes all Fe in the bulk compositions to be FeO.

P-T conditions during M_1

Temperature during the M_1 peak of metamorphism is constrained by the biotite melting reactions. Experimental studies investigating the fluid-absent melting behaviour of biotite in natural metapelites and metagreywackes indicate that, for a wide range of pressures, melting will begin between 780 and 830 °C (Stevens et al., 1995) (Fig. 7). Extensive melt production (>30 vol%) will not occur at a temperature lower than 875 to 900 °C. Biotite coexists with H_2O -undersaturated granitic melt and the restitic assemblage to temperatures between 875 and 920 °C, depending on αAl_2O_3 and the bulk rock Mg# (Stevens, 1995). These data suggest that the migmatitic metapelites in this study equilibrated at temperatures of at least 850 °C. The restitic samples most likely equilibrated at a temperature in excess of 920 °C.

M_1 pressure can be constrained by the assemblage garnet + cordierite + orthopyroxene + quartz in the metagreywacke migmatites. This assemblage has equilibrated within the divariant reaction field of the equilibrium $Grt + Qtz = Crd + Opx$, and is a useful geobarometer (e.g. Perchuk and Lavrentéva, 1983). The compositions of the relevant phases were measured using EDS analysis and the Link EXL system on the JEOL JSM 6400 SEM in the Geology Department at Manchester University. All probe analyses were carried out using an accelerating voltage of 15kV and a probe current of 1.5nA; a counting time of 40s was used. The results are presented in the Appendix. Mineral component activities were calculated using the program RECALC of Roger Powell and thermobarometry calculations were performed using the program THERMOCALC of Powell and Holland (1988) and the extended dataset of Holland and Powell (1990). Calculations using the core compositions of garnet, cordierite and orthopyroxene from sample VT596 suggest pressures during M_1 of 0.48 ± 0.13 GPa and 0.51 ± 0.16 GPa at 800 and 900°C respectively. Similarly, data from sample GS4 indicate pressures of 0.52 ± 0.09 GPa and 0.56 ± 0.13 GPa at the same temperatures.

Prograde conditions

In many of the samples studied the biotite incongruent melting reactions consumed sillimanite and produced garnet, as indicated by abundant corroded sillimanite inclusions in garnet. Other inclusions in garnet hint at the possible existence of a lower-pressure, high-temperature assemblage during the high-temperature prograde evolution. Garnet crystals in the garnet-quartz restites occasionally contain corroded inclusions of green, hercynitic spinel and cordierite in addition to sillimanite, and in several cases inclusions of spinel in contact with quartz have been found (Fig. 8). The high-temperature, low-pressure granulite facies boundary is marked by the transition from garnet-sillimanite-quartz assemblages to spinel-cordierite-quartz assemblages (Waters, 1991). It appears, thus, that the Vredefort granulites evolved through this boundary in a reverse sense, i.e. from spinel-cordierite assemblages to garnet-sillimanite assemblages during their anatetic history. If this interpretation is correct, the experimentally determined positive slope on the transition to spinel-cordierite-quartz assemblages implies an anti-clockwise P - T path. In the simple FMASH system the garnet-producing reaction results in excess Al_2SiO_5 . Observations in the present samples indicate that garnet grew at the expense of sillimanite and spinel. This is possible, as in the samples under investigation a concurrent incongruent biotite melting reaction was also producing garnet and an aluminous, H_2O -undersaturated melt.

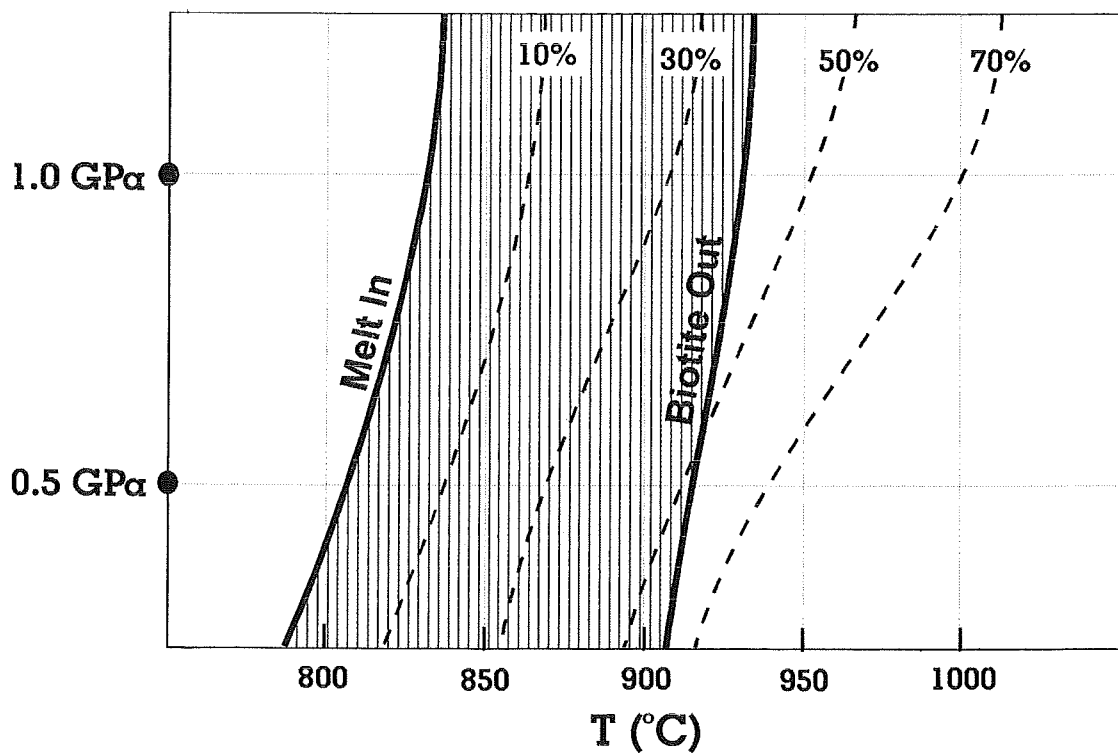


Figure 7: The experimentally determined temperature range of biotite fluid-absent melting in metagreywacke (from Stevens, 1995). The experiments used a natural titaniferous biotite (~2.5 wt% TiO_2) with $\text{Mg}\# = 58$ extracted from an amphibolite-grade metapelite. The hatched area represents the field of biotite-melt coexistence, the dashed lines are contours of melt proportion. Note that although minor migmatisation begins close to 800 °C, extensive melting only occurs at temperatures > 850 °C. Anhydrous, biotite-free restites are only produced following melt extraction from rocks heated to > 900 °C.

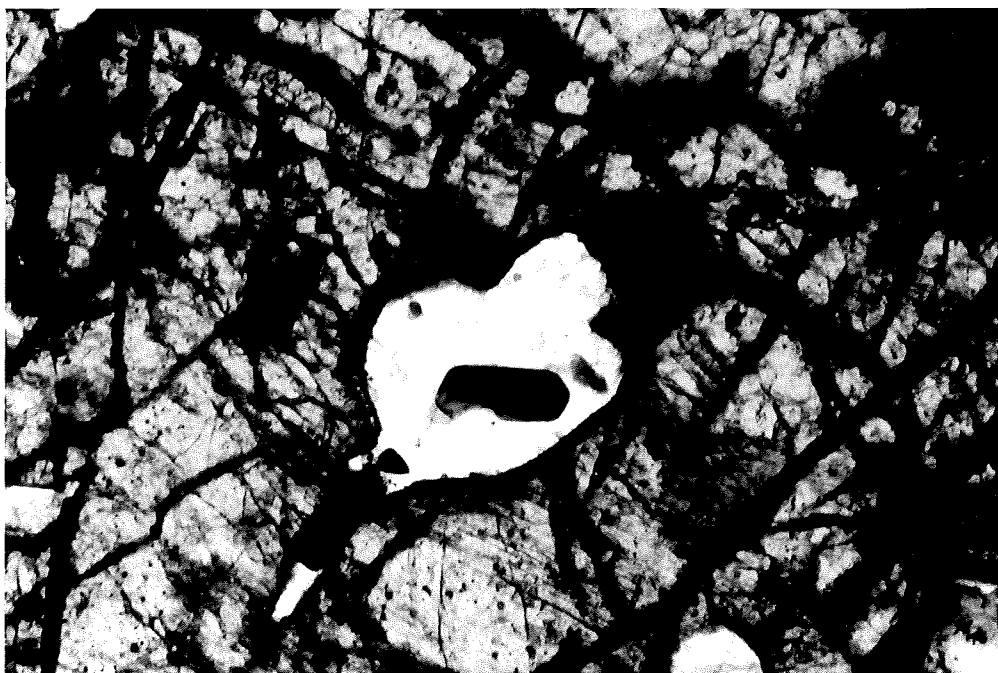


Figure 8: Inclusion of the diagnostic high-temperature, low-pressure granulite facies association of hercynitic spinel and quartz in a garnet of the garnet-quartz resite (Sample V600). These garnets also contain inclusions of sillimanite and occasionally cordierite. The spinel inclusion in quartz is clearly visible in the centre of the photograph. The long axis of the photograph represents 2.5 mm.

Cooling from the metamorphic peak

The P - T evolution in the period following M_1 is marked by the development of a retrograde reaction texture in the migmatised rocks. Cordierite, produced by the biotite melting reactions, has been partially replaced by biotite and sillimanite through a crystallisation-hydration reaction ($\text{Melt} + \text{Crd} = \text{Bt} + \text{Sil} + \text{Qtz}$) driven by rising $a\text{H}_2\text{O}$ in the melt during the cooling and partial crystallisation of the leucosomes. The involvement of an externally derived fluid, causing a general rise in $a\text{H}_2\text{O}$, is unlikely as cordierite in restitic rocks that had lost all their melt is often in contact with K-feldspar, yet has not reacted to biotite. The precise conditions of the retrogression are difficult to constrain. Garnet-biotite thermometry would be the most suitable method for estimating the temperature towards the end of the M_2 cooling period. However, the resultant biotite-sillimanite intergrowths and the rims of the large garnet crystals have been overprinted by subsequent post-shock M_3 metamorphism. As a result, the compositions that existed at the end of M_2 are impossible to determine confidently. However, the fact that melt was a likely reactant implies that the reaction occurred on the cooling path between the peak of metamorphism and the H_2O saturated granite solidus ($\sim 650^\circ\text{C}$). The high-grade nature of the M_2 retrogression is also supported by the titaniferous nature of the resultant biotite (Table 4 of the Appendix). There are no textures indicating the concurrent breakdown or growth of garnet through pressure-sensitive equilibria. Thus, it appears that cooling was approximately isobaric.

M_3 , POST-SHOCK METAMORPHISM

The well-documented Vredefort shock metamorphic features are also manifested in the rocks of the present study, the most typical and obvious elements being pseudotachylite veinlets. These veinlets are, in turn, overprinted by metamorphic textures developed after the shock deformation

event and the formation of the Dome. Pseudotachylite formation pre-dates the formation of second-generation cordierite and orthopyroxene coronas around garnet (Fig. 9), as well as the replacement of the sillimanite + cordierite assemblage that resulted from the crystallisation-hydration reaction by a spinel + orthopyroxene assemblage (Figs. 10 and 11). Pseudotachylite material has also recrystallised to high grade assemblages that includes orthopyroxene, cordierite and biotite (Fig. 12). As the M_3 assemblages post-date shock features that appear to be the result of a meteorite impact, the possibilities for $P-T$ evolution trends and rates are far wider than those usually considered for "normal" metamorphic processes. The M_3 textures are generally very fine grained and the average grain size is often $< 15\mu\text{m}$. However, there is a degree of variation in the grain size of the cordierite-orthopyroxene symplectites, and in the extent of garnet replacement by these textures. This possibly reflects different degrees of overstepping of the reaction $\text{Grt} + \text{Qtz} = \text{Crd} + \text{Opx}$, i.e. it correlates with bulk rock Mg#. However, it may also reflect differences in M_3 temperature due to pre-shock metamorphic gradients (the melting relations do appear to record a peak-temperature gradient in rocks currently exposed at surface). In the case of the most fine-grained coronas, no zonation is observed in the garnet adjoining the symplectite and it is not possible to determine the garnet composition in equilibrium with these reaction products (e.g. sample VT596 in Table 2). However, in the case of the coarsest, best-developed corona intergrowths (Fig. 13) there is a clear zonation to more Fe-rich compositions at the garnet rim (e.g. sample VT206 in Table 2). In these samples a reasonable case can be made for a local approach to equilibrium during M_3 . In this case, the garnet rim composition and the compositions of the cordierite and orthopyroxene intergrown in the symplectite have been applied using the same geobarometer as applied to the M_1 assemblage, resulting in a pressure estimate that ranges between $0.27 \pm 0.08 \text{ GPa}$ at 700°C and $0.33 \pm 0.13 \text{ GPa}$ at 900°C .

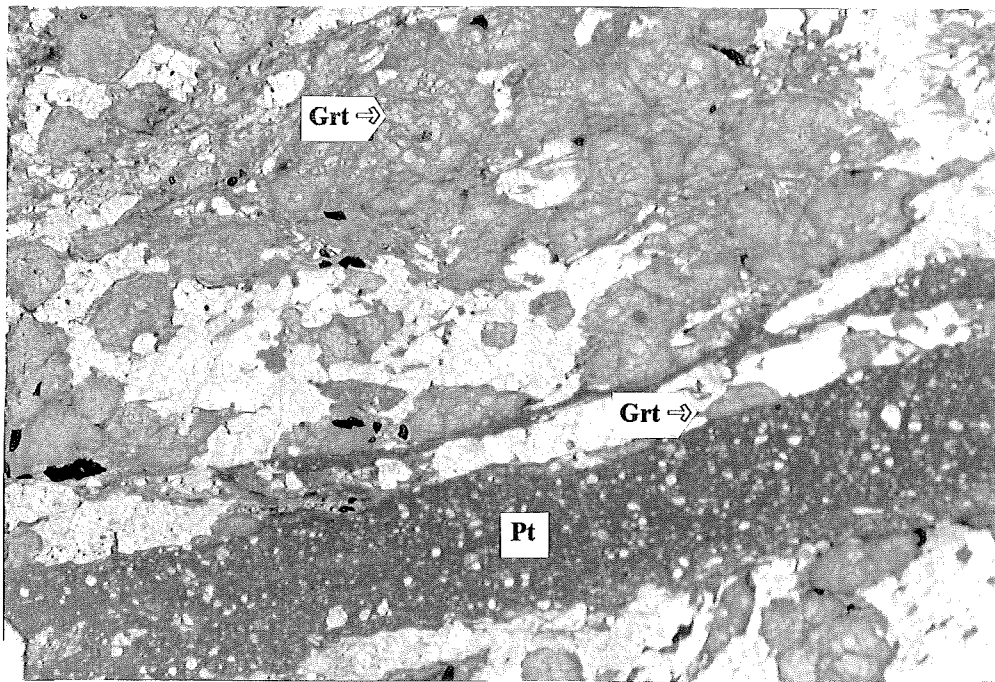


Figure 9: Pseudotachylite (Pt) truncating M_1 garnet (Grt) in the garnet-quartz restite. The dark, anastomosing areas around the garnet crystals (best visible in the upper central portion) are fractures filled with very fine grained cordierite + orthopyroxene symplectites. Where these zones are developed adjacent to the pseudotachylite they are undeformed indicating that M_3 postdated the shock event (see also Schreyer, 1983). The long axis of the photograph represents 14 mm.

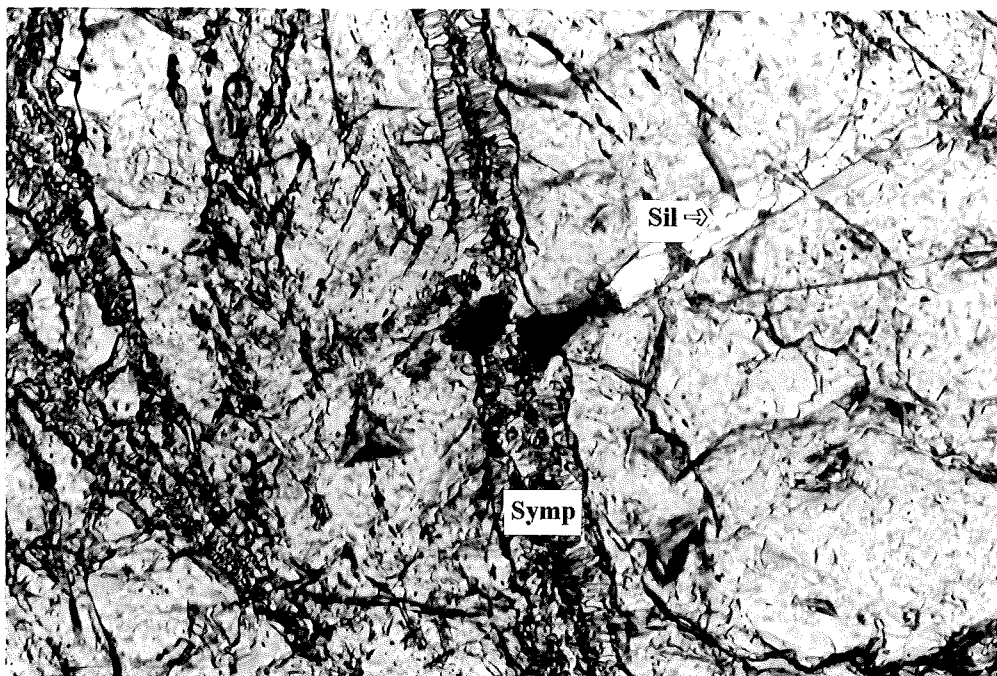


Figure 10: Sillimanite (Sil) inclusion in garnet that has been partially replaced by spinel. The spinel has only been produced where the sillimanite has come into contact with cordierite through the breakdown of garnet to cordierite + orthopyroxene symplectite (Symp) during M_3 . The long axis of the photograph represents 3 mm.

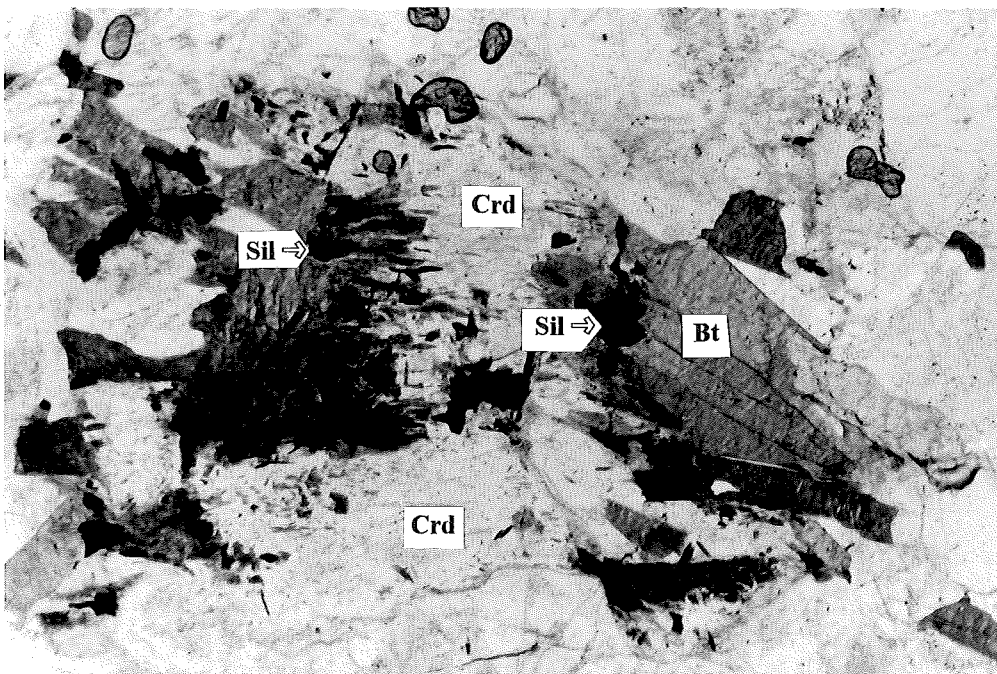


Figure 11: The M_2 retrogression texture. Cordierite (Crd) has been partially replaced by biotite (Bt) and sillimanite (Sil). The sillimanite has subsequently been pseudomorphously replaced by aggregates of spinel and orthopyroxene during M_3 . This results in the opaque appearance of the needles. The long axis of the photograph represents 5 mm.

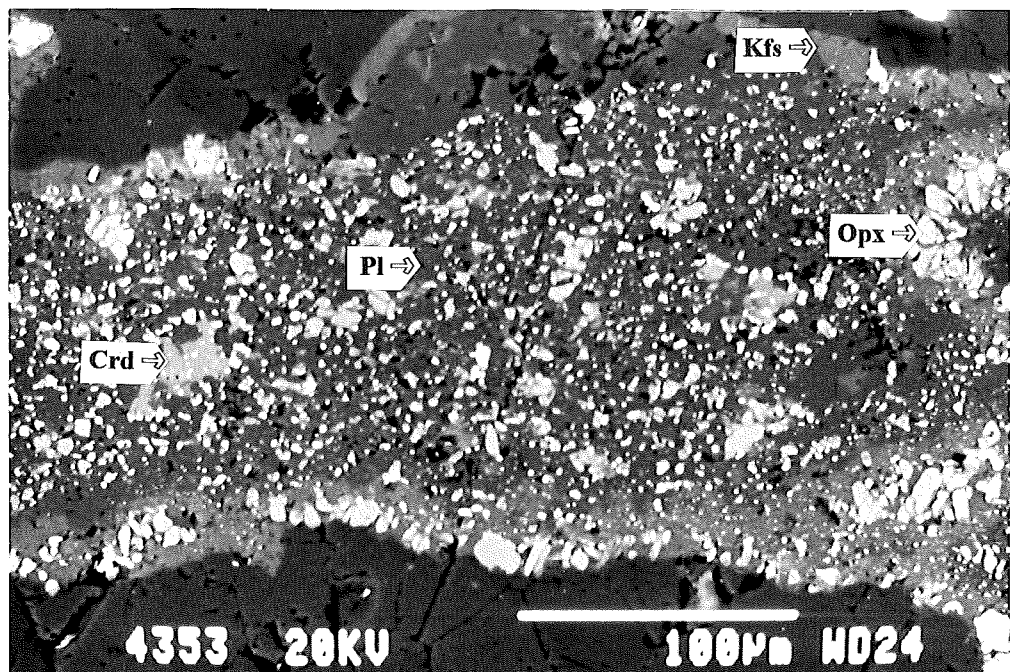


Figure 12: Backscattered electron SEM image of pseudotachylite. The pseudotachylite glass has recrystallized to plagioclase (Pl), K-feldspar (Kfs), orthopyroxene (Opx) and cordierite (Crd), indicating the high grade nature of the post-shock M_3 overprint.

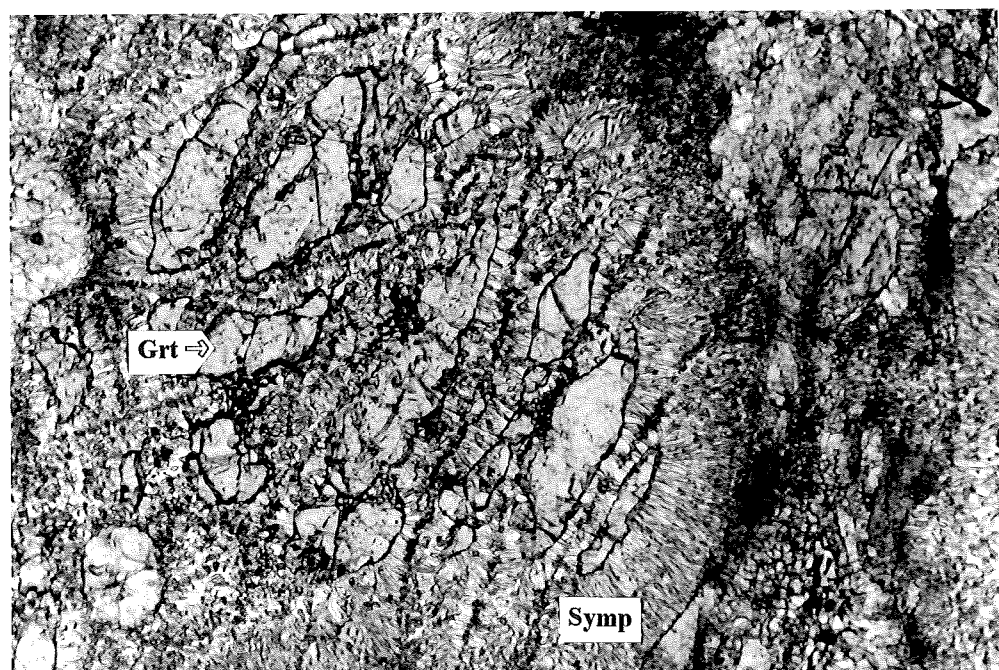


Figure 13: Example of the most coarse-grained symplectites (Symp) of cordierite and orthopyroxene around relic garnet (Grt) from sample V206. In this case the garnet crystal is clearly zoned to more Fe-rich rim compositions (Appendix, Table 1). The long axis of the photograph represents approximately 2 mm.

The temperature during M_3 is difficult to determine. Clearly the assemblage of cordierite, sillimanite and quartz became unstable and was replaced by cordierite, spinel and quartz assemblages. If this represents an equilibrium phase transition then temperatures similar to those of M_1 are indicated. However, the maximum temperature is constrained to below 900 °C by the preservation of many biotite-quartz intergrowths resulting from the M_2 retrogression. These suggest that the M_3 temperatures did not exceed those for fluid-absent melting of biotite + quartz as determined by Vielzeuf and Clemens (1992). A minimum temperature of 680 to 700 °C, slightly above the minimum granite solidus at 0.25 GPa, is corroborated by the presence of the undeformed Central Anatetic Granite that is believed to have been a partial melt at the time of the formation of the Dome (Hart *et al.*, 1981). This granite is characterised by a total lack of the planar deformation features in quartz that typify the Vredefort basement (Fig. 14). Also, some leucosomes in the ILG are characterised by textures that appear to indicate quenching of granitic magma through rapid decompression or cooling following dome formation (Fig. 15). Quartz in these leucosomes also lacks planar deformation features.

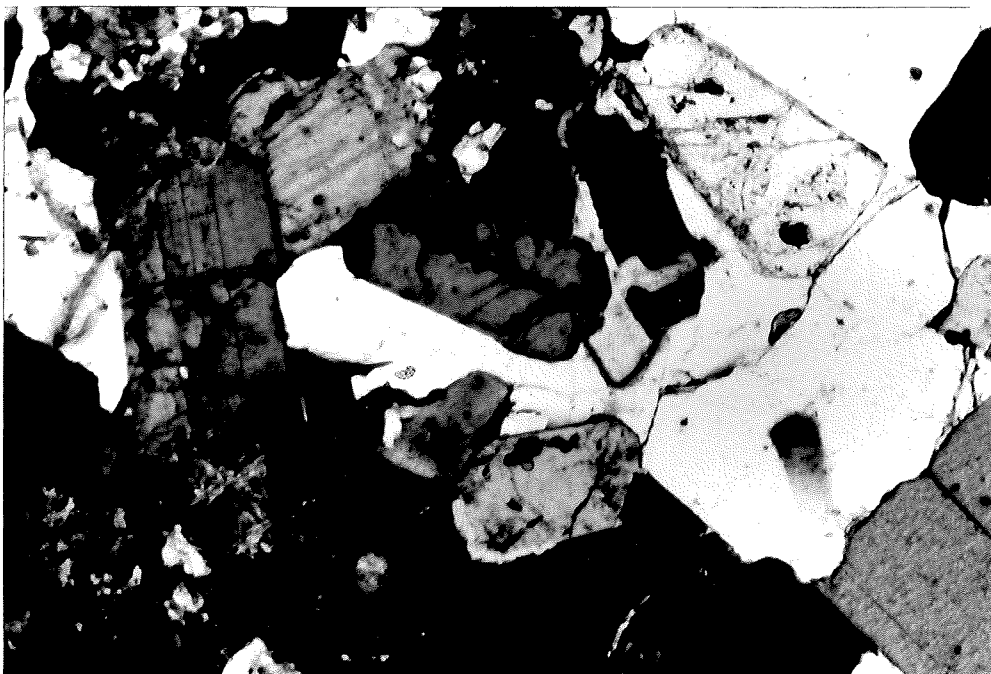


Figure 14: The microtexture of the Central Anatetic Granite. The internal texture of this rock does not record the shock deformation features (planar deformation features etc.) present in most of the core basement. The long axis of the photograph represents 5 mm.



Figure 15: The microtexture of a representative leucosome from within the ILG. The radiating clusters of plagioclase crystals (Pl) are considered to represent quench features. These leucosomes also contain no evidence of shock deformation.

ORIGIN OF THE METAMORPHISM

The pre-shock P - T evolution, documented by the prograde M_1 and M_2 textures, defines a mid-crustal, anti-clockwise P - T loop (Fig. 16). This type of metamorphic evolution can result from the tectonic thickening of previously thinned, hot crust (Vielzeuf and Kornprobst, 1984); catastrophic thinning of the underlying mantle during tectonic thickening of the crust (e.g. Sandiford and Powell, 1986; Loosveld, 1989); or, extrusion or intrusion of voluminous high-level magmas during regional heating (Wells, 1980; Bohlen, 1987). The preservation of the Witwatersrand Supergroup and younger cover sequences in the area surrounding the Vredefort Dome rules out major tectonics as a driving mechanism in the granulite facies metamorphism of the Vredefort Basement since the beginning of sedimentation in the Witwatersrand Basin at approximately 3.07 Ga (Robb and Meyer, 1995). Thus, the pre-shock P - T loop documented in this study either relates to tectonically driven metamorphism predating Witwatersrand sedimentation or it is the product of anorogenic magmatism in the crust. The abundance of restitic metapelitic compositions produced during the peak of metamorphism (M_1) indicates that the temperature attained by many of the rocks exposed in the core exceeded 900 °C. These metamorphic conditions are not possible in the crust (particularly the mid-crust) without the addition of substantial amounts of mantle heat (Wells, 1980; Ashwal *et al.*, 1992). This argues strongly for a magmatic source of heat as the driving mechanism for the formation of the granulites.

The P - T loop documented in this study (Fig. 16) is identical in form to that proposed for the amphibolite facies metapelites of the Witwatersrand Supergroup exposed in the collar of the Dome by Gibson and Wallmach (1995) (Fig. 4). This indicates that the metamorphism in both the core and the collar are linked to the same post-Witwatersrand, pre-Vredefort Dome

thermomagmatic event. The Kaapvaal Craton experienced three major magmatic events between Witwatersrand times and the formation of the Vredefort Dome: the Ventersdorp Supergroup lavas at 2.71 Ga (Armstrong *et al.*, 1991); the extrusion of the Hekpoort andesites of the Transvaal Supergroup at 2.25 Ga (Eriksson *et al.*, 1995); and the major magmatic event that produced both the predominantly rhyolitic volcanics of the Rooiberg Group, capping the Transvaal Supergroup, and the Bushveld Complex (Eriksson *et al.*, 1995; Twist and French, 1983) at approximately 2.06 Ga (Walraven and Hattingh, 1993). The Bushveld Complex event appears to be the most likely alternative for several reasons. The rhyolite volcanism that accompanied the intrusion of the mafic phase of the Bushveld Complex, and the granites associated with the Complex, clearly indicate extensive high temperature crustal anatexis and thus, crustal granulite formation, associated with this event. The present erosional remnants of the Rooiberg Group indicate a thickness of at least 5000 m for the extrusive component (Eriksson *et al.*, 1995). Thus, if Rooiberg-type rhyolites were derived from the crust below the present levels exposed in the Vredefort core, or the Bushveld Complex originally extended over this area, or both, this magmatic activity could account for the observed high-temperatures of metamorphism as well as the synchronous burial of mid-crustal levels indicated by the anticlockwise *P-T* loop.

An age of metamorphism relatively close to that of doming is also supported by other data. The post-shock M_3 metamorphism overprints the products of a single high-grade retrogression reaction that consumed cordierite + melt and produced biotite + sillimanite. No pre- M_3 lower grade retrogression features have been observed. The M_3 metamorphism thus appears to reflect the decompression of already hot rocks induced by the 2.02 meteorite impact. The data in this study suggest some 9 km of rapid (near-instantaneous) uplift and exhumation of rocks at a temperature not lower than approximately 700 °C. This minimum temperature is constrained by both the high-grade nature of the M_3 equilibria and the presence of the Central Anatetic Granite and granitic leucosomes within the core migmatites, which are not deformed by the shock features. A post-impact thermal effect, due to post-shock heating of the terrane related to the relaxation of shock-induced strain in mineral lattices (e.g., Raikes and Ahrens, 1979) has been suggested for the Vredefort Dome (Grieve *et al.*, 1990). Such effects possibly resulted in a local increase in temperature in some rocks during M_3 . However, the dominant M_3 overprint appears to be one of decompression and quenching as illustrated by the minute grain size of the resultant cordierite-orthopyroxene symplectites and the quench textures in some leucosomes.

The minimum temperature constraint for M_3 implies a geothermal gradient of at least 39 °C/km prior to the Vredefort event at 2.02 Ga - significantly higher than expected for stable cratonic crust (e.g. Hyndman *et al.*, 1968) because the terrane was still cooling from the peak of metamorphism. The geochronological data suggest a 30 to 40 Ma gap between Bushveld magmatism and Dome formation (Walraven and Hattingh, 1993; Kamo *et al.*, 1995). This constrains the cooling rate in the granulites to between 8 and 10 °C/Ma. Such long-lived high-temperature events are known from other terranes. In the low-pressure granulite facies metapelites of the Reynolds Range, Australia, diachronous zircon mineral ages in granitic leucosomes (Collins and Williams, 1995) have been interpreted by Williams *et al.* (1996) as indicative of slow cooling to the granite solidus following peak metamorphic conditions, over a period of at least 26 Ma. Even assuming no M_3 heating through impact-related phenomena, the rapid decompression of the core to ~ 0.22 Gpa would have converted the predomining geothermal gradient of ~ 39 °C/km to one of ~ 87 °C/km. This is grossly out of equilibrium with the thermal state of the upper cratonic crust and probably resulted in very rapid cooling following M_3 .

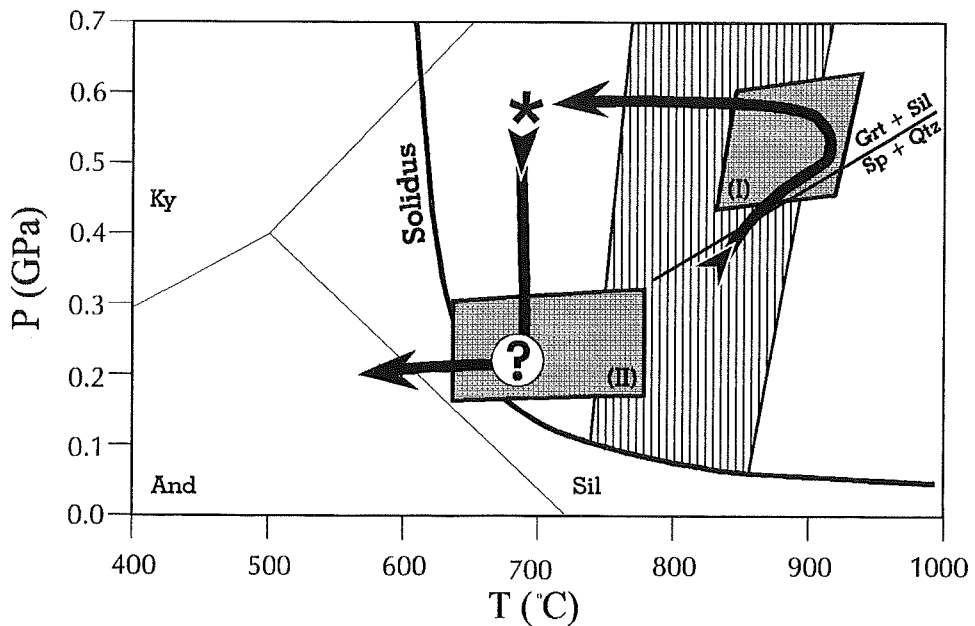


Figure 16: Proposed P-T loop for the Vredefort granulites. The form of the loop and the magnitude of the peak conditions constrain the mechanism of granulite formation to intraplating of mantle-derived magmas. Boxes (I) and (II) represent the P-T conditions calculated for the granulite and post-pseudotachylite assemblages respectively. The large hatched field is the experimentally determined field of biotite-melt coexistence from the data of Stevens et al. (1995). The asterisk represents the Vredefort Catastrophe and the main phase of pseudotachylite formation. Uplift and cooling after the Vredefort Catastrophe at 2.02 Ga must have been extremely rapid, but the exact temperature at the time of equilibration of the assemblages represented by box (II) is difficult to constrain due to the minute equilibration domain size during this event.

CONCLUSIONS

The metapelitic granulites exposed in the core of the Vredefort Dome preserve evidence of an anticlockwise P-T loop and a two-stage metamorphic history divided by shock deformation resulting from the Vredefort catastrophe at ~2.02 Ga. This shock event followed the partial retrogression of the granulites, suggesting that M₁ predated the formation of the Dome at 2.02 Ga by at least tens of millions of years. Thus, it is unlikely that there is a genetic link between dome formation and the granulite-grade metamorphism. The M₁ metamorphism is interpreted as an anorogenic, mid-crustal anatexic episode resulting from heat advected to the crust through intraplating/underplating during the 2.06 Ga Bushveld magmatic event. The preservation of both biotite-bearing migmatites and anhydrous restites from the core suggests that the temperature in the granitic magma derived from these rocks would not have departed dramatically from the 850–900 °C buffered by biotite-melt coexistence. Consequently, the core granulites are not candidates for the protoliths of the Rooiberg felsites – these must derive from a zone of more intimate mantle magma-crust interaction. The fine-grained cordierite-orthopyroxene symplectites found rimming garnet developed after the shock deformation event. Mineral compositions in these intergrowths record decompression from the pressures of the peak of metamorphism, equivalent to ~9 km of

exhumation. It is proposed that this decompression occurred almost instantaneously through the cratering process resulting from a large meteorite strike. The deepest levels exhumed in the crater fortuitously sampled the upper, mid-crustal, portions of a slowly cooling granulite terrane giving an unique insight into the ~2.06 Ga granulite terrane that probably underlies a large portion of the central Kaapvaal Craton.

ACKNOWLEDGEMENTS

D. Stepto is acknowledged for providing some of the sample material used in this study and for assistance in finding specific field localities. RLG acknowledges a University of the Witwatersrand URC grant.

REFERENCES

- Allsopp, H.L., Fitch, F.J., Miller, J.A. and Reimold, W.U., 1991, $^{40}\text{Ar}/^{39}\text{Ar}$ stepheating age determinations relevant to the formation of the Vredefort Dome, South Africa. *South African Journal of Science*, **87**: 431-442.
- Armstrong, R.A., Compston, W., Retief, E.A., Williams, I.S. and Welke, H.I., 1991, Zircon ion-microprobe studies bearing on the age and evolution of the Witwatersrand Triad. *Precambrian Research*, **53**: 243-266.
- Ashwal, L.D., Morgan, P. and Hoisch, T.D., 1992, Tectonics and heat sources for granulite metamorphism of supracrustal-bearing terranes. *Precambrian Research*, **55**: 525-538.
- Ashworth, J. R., 1985, Introduction to migmatites. In, Ashworth, J. R. (ed), *Migmatites*, Blackie and Son, Glasgow, U.K., p. 1-35.
- Bisschoff, A. A., 1972, Tholeitic intrusions in the Vredefort Dome. *Transactions of the Geological Society of South Africa*, **75**: 23-34.
- Bisschoff, A. A., 1982, Thermal metamorphism in the Vredefort Dome. *Transactions of the Geological Society of South Africa*, **85**: 43-57.
- Bohlen, S.R., 1989, Pressure-temperature-time paths and a tectonic model for the evolution of granulites. *Journal of Geology*, **95**: 617-632.
- Clemens, J.D., 1990, The granulite-granite connection. In: Vielzeuf, D. and Vidal, Ph. (eds), *Granulites and Crustal Evolution*, NATO ASI Series, Kluwer Academic Publishers, Dordrecht, 585 pp.
- Collins, I. and Williams, I.S., 1995, SHRIMP ion probe dating of short-lived Proterozoic tectonic cycles in the northern Arunta Inlier, central Australia. *Precambrian Research*, **71**: 69-89.
- Dawson, J. B. and Smith, J. V., 1987, Reduced sapphirine granulite xenoliths from the Lace Kimberlite, South Africa; implications for the deep structure of the Kaapvaal Craton. *Contributions to Mineralogy and Petrology*, **95**: 376-383.

- De Wit, M.J., Roering, C., Hart, R.J., Armstrong, R.A., De Ronde, C.E.J., Green, R.W.E., Tredoux, E.P., and Hart, R.A., 1992, Formation of an Archaean continent. *Nature*, **357**: 553-562.
- Droop, G.T.R. 1987. A general equation for estimating Fe³⁺ concentrations in ferromagnesian silicates and oxides from microprobe analyses, using stoichiometric criteria. *Mineralogical Magazine*, **51**: 431-435.
- Eriksson, P.G., Hattingh, P.J. and Alterman, W., 1995, An overview of the geology of the Transvaal Sequence and Bushveld Complex, South Africa. *Mineralium Deposita*, **30**: 98-111.
- French, B.M. and Nielsen, R.L., 1990, Vredefort bronzite granophyre: chemical evidence for origin as a meteorite impact melt. *Tectonophysics*, **171**: 119-138.
- Gibson, R.L. and Wallmach, T., 1995, Low pressure-high temperature metamorphism in the Vredefort Dome, South Africa: anticlockwise pressure-temperature path followed by rapid decompression. *Geological Journal*, **30**: 319-331.
- Grieve, R.A.F., Robertson, P.B. and Dence, M.R., 1981, Constraints on the formation of ring impact structures, based on terrestrial data. In: Schultz, P.H. and Merrill, R.B. (eds), *Multi-Ring Basins*. Pergamon Press, Oxford, 37-57.
- Grieve, R.A.F., Coderre, J.M., Robertson, P.B. and Alexopoulos, 1990, Microscopic planar deformation features in quartz of the Vredefort Structure: Anomalous but still suggestive of an impact origin. *Tectonophysics*, **171**: 185-200.
- Harley, S.L., 1989, The origins of granulites: a metamorphic perspective. *Geological Magazine*, **126**: 215-331.
- Hart, R.J., 1978, A study of the isotopic and geochemical gradients in the Vredefort Structure, with implications for continental heat flow. Ph.D. Thesis (unpublished), University of the Witwatersrand, Johannesburg, 172 pp.
- Hart, R.J., Welke, H.J. and Nicolaysen, L.O., 1981, Geochronology of the deep profile through Archaean basement at Vredefort, with implications for early crustal evolution. *Journal of Geophysical Research*, **86**: 10630-10680.
- Hart, J. R. and Nicolaysen, L. O. (eds), 1981, *Excursion Guide Book for the Geology of the Vredefort Structure*. South African Geodynamics Project, Geological Society of South Africa, 64 pp.
- Hatton, C. J. and Schweitzer, J. K., 1996. Evidence for synchronous extrusive and intrusive Bushveld magmatism. *Journal of African Earth Science*, in press.
- Holland, T. J. B. and Powell, R., 1990, An enlarged and updated internally consistent thermodynamic dataset with uncertainties and correlations: the system K₂O-Na₂O-CaO-MgO-MnO-FeO-Fe₂O₃-Al₂O₃-TiO₂-SiO₂-C-H₂-O₂. *Journal of Metamorphic Geology*, **8**:

89-124.

- Hyndman, R.D., Lambert, I.B., Heier, H.S., Jaeger, J.C. and Ringwood, A.E., 1968, Heat flow and surface radioactivity in the Precambrian Shield of Western Australia. *Journal of the Physics of the Earth and Planetary Interiors*, **1**: 129-135.
- Kamo, S.L., Reimold, W.U., Krogh, T.E. and Colliston, W.P., 1995, Shocked zircons in Vredefort pseudotachylite and the U-Pb zircon age of the Vredefort impact event. *Centennial Geocongress of the Geological Society of South Africa*. Abstract volume 1, 566-569.
- Loosveld, R.J.H., 1989, The synchronism of crustal thickening and low-pressure facies metamorphism in the Mount Isa Inlier, Australia. 2. Fast convective thinning of mantle lithosphere during crustal thickening. *Tectonophysics*, **165**: 191-218.
- Nel, L.T., 1927, The geology of the country around Vredefort. *Special Publication of the Geological Survey of South Africa*, **6**: 134 pp.
- Nicolaysen, L. O., Burger, A. J. and Van Niekerk, C. B., 1963, The origin of the Vredefort structure in the light of new isotopic data. (Abstract) *International Union Geodesy Geophysics 13th General Assembly*, Berkeley, California.
- Martini, J.E.J., 1992, The metamorphic history of the Vredefort Dome at approximately 2 Ga as revealed by coesite-stishovite-bearing pseudotachylites: *Journal of Metamorphic Geology*, **10**: 517-527.
- McCarthy, T.S., Charlesworth, E.G. and Stanistreet, I.G., 1986, Post-Transvaal structural features of the northern portion of the Witwatersrand Basin. *Transactions of the Geological Society of South Africa*, **89**: 311-324.
- McCarthy, T.S., Stanistreet, I.G. and Robb, L.J. 1990, Geological studies related to the origin of the Witwatersrand Basin and its mineralization - an introduction and a strategy for research and exploration. *South African Journal of Geology*, **93**: 1-4.
- Perchuk, L.L. and Lavrentéva, I.V., 1983, Experimental investigation of exchange equilibria in the system cordierite-garnet-biotite. *In: Saxene, S.K. (ed), Kinetics and Equilibrium in Mineral Reactions*. Springer-Verlag, New York, 199-240.
- Powell, R. and Holland, T. J. B., 1988, An internally consistent dataset with uncertainties and correlations: 3. Applications to geobarometry, worked examples and a computer program. *Journal of Metamorphic Geology*, **6**: 173-204.
- Powell, R. and Downes, J., 1990, Garnet porphyroblast-bearing leucosomes in metapelites: mechanisms, phase diagrams, and an example from Broken Hill, Australia. *In, Ashworth, J. R. and Brown, M. (eds), High-Temperature Metamorphism and Crustal Anatexis*. Unwin-Hyman, London, 105-123.
- Raikes, S.A. and Ahrens, T.S., 1979, Post-shock temperatures in minerals. *Geophysical Journal of the Royal Astronomical Society*, **58**: 717-747.

- Reimold, W.U., 1993, A review of the geology and deformation related to the Vredefort structure, South Africa. *Journal of Geological Education*, **41**: 106-117.
- Robb, L.J. and Meyer, F.M., 1995, The Witwatersrand Basin, South Africa: Geological framework and mineralization processes. *Economic Geology Research Unit Information Circular*. University of the Witwatersrand, Johannesburg, **293**, 36 pp.
- Roering, C. and Smit, C.A., 1987, Bedding-parallel shear, thrusting and quartz vein formation in Witwatersrand quartzites. *Journal of Structural Geology*, **9**, 419-427.
- Sandiford, M. and Powell, R., 1986, Deep crustal metamorphism during continental extension: modern and ancient examples. *Earth and Planetary Science Letters*, **79**: 151-158.
- Schreyer, W., Abraham, K. and Mueller, W.F., 1978, Clinoeulite (magnesian clinoferro-sillite) in a eulysite of a metamorphosed iron formation in the Vredefort Structure, South Africa. *Contributions to Mineralogy and Petrology*, **65**: 351-361.
- Schreyer, W. and Abraham, K., 1978, Symplectic cordierite-orthopyroxene-garnet assemblages as products of contact metamorphism of pre-existing basement granulites in the Vredefort Structure, South Africa, and their relations to pseudotachylite. *Contributions to Mineralogy and Petrology*, **68**: 53-62.
- Schreyer, W., 1983, Metamorphism and fluid inclusions in the basement of the Vredefort Dome, South Africa: Guidelines to the origin of the structure. *Journal of Petrology*, **24**: 26-47.
- Spray, J.G., Kelley, S.P. and Reimold, W.U., 1995, Lazer-probe ^{40}Ar - ^{39}Ar dating of pseudotachylites and the age of the Vredefort impact event. *Meteoritics*, **30**: 335-343.
- Srogi, L., Wagner, M. E. and Lutz, T.M., 1993, Dehydration partial melting and disequilibrium in the granulite-facies Wilmington Complex, Pennsylvania-Delaware Piedmont. *American Journal of Science*, **293**: 405-462.
- Stepto, D., 1979, A geological and geophysical study of the central portion of the Vredefort Dome Structure. Ph.D. Thesis (unpubl), University of the Witwatersrand, Johannesburg, South Africa, 3 vol, 642 pp.
- Stepto, D., 1990, The geology and gravity field in the central core of the Vredefort Structure. *Tectonophysics*, **171**: 75-103.
- Stevens, G. and Van Reenen, D.D., 1992, Partial melting and the origin of the metapelitic granulites in the Southern Marginal Zone of the Limpopo Belt, South Africa. *Precambrian Research*, **55**: 303-319.
- Stevens, G., Clemens, J.D. and Droop, G.T.R., 1995, Hydrous cordierite in granulites and crustal magma production. *Geology*, **23**: 925-928.
- Stevens, G., 1995, Compositional controls on partial melting in high-grade metapelites; a

- petrological and experimental study. Ph.D. Thesis (unpubl), University of Manchester, 243 pp.
- Therriault, A.M., Ried, A.M. and Reimold, W.U., 1993, Original size of the Vredefort Structure, South Africa. *Lunar Planetary Science*, **24**: 1419-1420.
- Trieloff, M., Reimold, W.U., Kunz, J., Boer, R.H. and Jessberger, E.K., 1994, ^{40}Ar - ^{39}Ar thermochronology of pseudotachylites at the Ventersdorp Contact Reef, Witwatersrand Basin. *South African Journal of Geology*, **97**: 365-384.
- Twist, D. and French, B.M., 1983, Voluminous acid volcanism in the Bushveld Complex: a review of the Rooiberg Felsite. *Bulletin of Volcanology*, **46**: 225-242.
- Vielzeuf, D. and Clemens, J. D., 1992, The fluid-absent melting of phlogopite + quartz: experiments and models. *American Mineralogist*, **77**: 1206-1222.
- Vielzeuf, D. and Kornprobst, J., 1984, Crustal splitting and the emplacement of Pyrenean Iherzolites and granulites. *Earth and Planetary Science Letters*, **67**: 87-96.
- Vielzeuf, D. and Montel, J-M., 1994, Partial melting of metagreywackes. 1. Fluid-absent experiments and phase relationships. *Contributions to Mineralogy and Petrology*, **117**: 375-393.
- Waters, D. J., 1991, Hercynite-quartz granulites, phase relations, and implications for crustal processes. *European Journal of Mineralogy*, **3**: 367-386.
- Walraven, F., Armstrong, R.A. and Kruger, F.J., 1990. A chronostratigraphic framework for the north-central Kaapvaal Craton, the Bushveld Complex and the Vredefort Structure. *Tectonophysics*, **171**: 23-48.
- Walraven, F. and Elsenbroek, J.H., 1991, Geochronology of the Schurwedraai alkali granite and associated nepheline syenite and implications for the origin of the Vredefort Structure. *South African Journal of Geology*, **94**: 228-235.
- Walraven, F. and Hattingh, E., 1993, Geochronology of the Nebo Granite, Bushveld Complex. *South African Journal of Geology*, **96**: 31-42.
- Wells, P.R.A., 1980, Thermal models for the magmatic accretion and subsequent metamorphism of continental crust. *Earth and Planetary Science Letters*, **46**: 253-265.
- Williams, I.S., Buick, I.S. and Cartwright, I., 1996, An extended episode of early Mesoproterozoic metamorphic fluid flow in the Reynolds Range, central Australia. *Journal of Metamorphic Geology*, **14**: 29-47.

APPENDIX

Table 1: Garnet compositions. The core compositions probably reflect equilibration during M₁. Garnet in all three of these samples is rimmed by M₃ symplectites, but only in VT206, where these are best developed, is there evidence for the equilibration of the garnet rim composition during this event. The Fe₂O₃ contents have been calculated according to the formulae of Droop (1987)

| | VT206 rim | VT206 10 | VT206 20 | VT206 60 | VT206 core | VT596 rim | VT596 core | VGS4 core |
|------------------------------------|--------------|-------------|-------------|-------------|---------------|--------------|---------------|--------------|
| SiO₂ | 36.83 | 36.38 | 35.99 | 36.70 | 36.41 | 38.03 | 37.82 | 38.78 |
| Al₂O₃ | 20.03 | 19.97 | 19.52 | 20.04 | 19.94 | 20.58 | 20.68 | 22.09 |
| Cr₂O₃ | 0.23 | 0.00 | 0.00 | 0.00 | 0.25 | 0.35 | 0.41 | 0.00 |
| Fe₂O₃ | 2.94 | 3.72 | 4.54 | 3.33 | 3.92 | 1.67 | 1.90 | 0.00 |
| FeO | 35.20 | 34.66 | 33.54 | 33.84 | 33.37 | 33.28 | 32.77 | 25.77 |
| MnO | 1.42 | 1.37 | 1.44 | 1.44 | 1.30 | 0.87 | 0.93 | 1.83 |
| MgO | 3.21 | 3.24 | 3.55 | 3.78 | 3.81 | 5.71 | 5.72 | 9.19 |
| CaO | 1.38 | 1.37 | 1.40 | 1.51 | 1.67 | 0.95 | 1.05 | 1.83 |
| Total | 101.24 | 100.71 | 99.98 | 100.64 | 100.67 | 101.44 | 101.28 | 99.49 |
| TSi | 5.91 | 5.87 | 5.85 | 5.90 | 5.85 | 5.97 | 5.94 | 5.99 |
| TAI | 0.09 | 0.129 | 0.15 | 0.10 | 0.15 | 0.03 | 0.06 | 0.01 |
| Sum T | 6.00 | 6.00 | 6.00 | 6.00 | 6.00 | 6.00 | 6.00 | 6.00 |
| Al^{IV} | 3.70 | 3.67 | 3.59 | 3.69 | 3.63 | 3.78 | 3.77 | 4.01 |
| Fe³ | 0.35 | 0.45 | 0.56 | 0.40 | 0.47 | 0.20 | 0.22 | 0.00 |
| Cr | 0.03 | 0.00 | 0.00 | 0.00 | 0.03 | 0.04 | 0.05 | 0.00 |
| Sum | 4.08 | 4.12 | 4.15 | 4.09 | 4.13 | 4.02 | 4.04 | 4.01 |
| Fe² | 4.72 | 4.68 | 4.56 | 4.55 | 4.49 | 4.37 | 4.31 | 3.33 |
| Mn | 0.19 | 0.19 | 0.20 | 0.20 | 0.18 | 0.12 | 0.12 | 0.24 |
| Mg | 0.77 | 0.78 | 0.86 | 0.91 | 0.91 | 1.34 | 1.35 | 2.12 |
| Ca | 0.24 | 0.24 | 0.24 | 0.26 | 0.29 | 0.16 | 0.18 | 0.30 |
| Sum B | 5.92 | 5.89 | 5.86 | 5.92 | 5.87 | 5.99 | 5.96 | 5.99 |
| Total | 16.00 | 16.01 | 16.01 | 16.01 | 16.00 | 16.01 | 16.00 | 16.00 |
| O | 24.00 | 24.00 | 24.00 | 24.00 | 24.00 | 24.00 | 24.00 | 24.00 |
| Mg# | 13.97 | 14.28 | 15.87 | 16.67 | 16.85 | 23.46 | 23.85 | 38.89 |

Table 2: Cordierite compositions. "Symp" = crystals in the M₃ cordierite-orthopyroxene symplectites. For VT596 these represent the composition of cordierite from symplectites around two different garnet crystals. "M₁" = coarse crystals from the peak metamorphic paragenesis. These compositions were determined on parts of the crystals that were well removed from areas with inclusions of M₃ generations of spinel or orthopyroxene

| | VT206 | VT596 | VT596 | VT596 | VGS4 |
|------------------------------------|--------------|-------------------|-------------------|----------------|----------------|
| | Symp | Symp ¹ | Symp ² | M ₁ | M ₁ |
| SiO₂ | 49.09 | 50.16 | 49.60 | 49.81 | 50.78 |
| Al₂O₃ | 32.16 | 33.05 | 32.28 | 34.12 | 33.17 |
| FeO | 11.20 | 5.59 | 5.97 | 4.48 | 4.00 |
| MgO | 7.15 | 9.97 | 10.11 | 10.84 | 10.96 |
| CaO | 0.00 | 0.11 | 0.00 | 0.00 | 0.00 |
| Na₂O | 0.00 | 0.00 | 0.36 | 0.31 | 0.34 |
| Total | 99.60 | 98.88 | 98.32 | 99.56 | 99.25 |
| Si | 5.05 | 5.06 | 5.05 | 4.98 | 5.07 |
| Al | 3.89 | 3.93 | 3.87 | 4.01 | 3.90 |
| Fe | 0.96 | 0.47 | 0.51 | 0.37 | 0.33 |
| Mg | 1.10 | 1.50 | 1.54 | 1.62 | 1.63 |
| Ca | 0.00 | 0.01 | 0.00 | 0.00 | 0.00 |
| Na | 0.00 | 0.00 | 0.07 | 0.06 | 0.07 |
| Total | 11.00 | 10.97 | 11.04 | 11.04 | 11.00 |
| O | 18.00 | 18.00 | 18.00 | 18.00 | 18.00 |
| Mg# | 53.40 | 76.14 | 75.12 | 81.41 | 83.16 |

Table 3: Orthopyroxene compositions. M₃ orthopyroxene; "Symp" = orthopyroxene in the symplectites around garnet; "Blocky" = orthopyroxene from the rims that surround the symplectites; "in crd" = orthopyroxene in cordierite that are associated with the M₃ production of spinel. Analyses labeled "M₁" are from coarse crystals that define the peak metamorphic paragenesis

| | VT206 | VT206 | VT596 | VT596 | VT596 | VGS4 |
|------------------------------------|-------|--------|--------|----------------|--------|----------------|
| | Symp | Blocky | Symp | M ₁ | in crd | M ₁ |
| SiO₂ | 46.38 | 47.26 | 50.83 | 50.77 | 51.68 | 52.73 |
| TiO₂ | 0.18 | 0.2 | 0 | 0 | 0 | 0 |
| Al₂O₃ | 3.17 | 3.13 | 3.17 | 3.12 | 1.85 | 5.36 |
| Cr₂O₃ | 0.33 | 0.22 | 0.23 | 0 | 0 | 0 |
| FeO | 38.22 | 38.83 | 27.57 | 28.75 | 26.97 | 21.1 |
| MnO | 0.38 | 0.38 | 0.37 | 0 | 0 | 0.42 |
| MgO | 10.23 | 10.26 | 17.36 | 16.92 | 18.21 | 19.96 |
| CaO | 0 | 0.25 | 0 | 0.16 | 0 | 0 |
| Na₂O | 0 | 0 | 0.43 | 0 | 0.31 | 0.43 |
| Total | 98.89 | 100.53 | 100.02 | 99.72 | 99.02 | 100 |
| Si | 1.89 | 1.9 | 1.94 | 1.96 | 1.99 | 1.96 |
| Ti | 0.01 | 0.01 | 0 | 0 | 0 | 0 |
| Al | 0.15 | 0.15 | 0.14 | 0.15 | 0.08 | 0.23 |
| Cr | 0.01 | 0.01 | 0.01 | 0 | 0 | 0 |
| Fe | 1.3 | 1.3 | 0.88 | 0.93 | 0.87 | 0.66 |
| Mn | 0.01 | 0.01 | 0.01 | 0 | 0 | 0.01 |
| Mg | 0.62 | 0.61 | 0.99 | 0.97 | 1.04 | 1.11 |
| Ca | 0 | 0.01 | 0 | 0.01 | 0 | 0 |
| Na | 0 | 0 | 0.03 | 0 | 0.02 | 0.03 |
| Total | 3.99 | 4 | 3.99 | 4.02 | 4 | 4 |
| O | 6 | 6 | 6 | 6 | 6 | 6 |
| Mg# | 32.29 | 31.94 | 52.80 | 51.05 | 54.45 | 62.71 |

Table 4: Biotite compositions produced during M₂ rehydration. OH per formula unit are assumed to be the ideal 2 for 24 oxygen

| | VT596 | VT596 |
|------------------------------------|-------|-------|
| SiO₂ | 37.70 | 37.30 |
| TiO₂ | 6.01 | 6.30 |
| Al₂O₃ | 14.75 | 15.41 |
| Cr₂O₃ | 0.67 | 0.69 |
| FeO | 14.12 | 13.62 |
| MgO | 14.12 | 13.81 |
| CaO | 0.18 | 0.16 |
| Na₂O | 0.37 | 0.00 |
| K₂O | 10.08 | 10.65 |
| H₂O | 1.97 | 1.97 |
| Total | 99.97 | 99.91 |
| Si | 5.74 | 5.68 |
| Al^{IV} | 2.26 | 2.32 |
| Al^{VI} | 0.38 | 0.44 |
| Ti | 0.69 | 0.72 |
| Cr | 0.08 | 0.08 |
| Fe | 1.80 | 1.73 |
| Mg | 3.20 | 3.13 |
| Ca | 0.03 | 0.03 |
| Na | 0.11 | 0.00 |
| K | 1.96 | 2.07 |
| Total | 16.25 | 16.20 |
| O | 24.00 | 24.00 |
| OH | 2.00 | 2.00 |
| Mg# | 64.00 | 64.40 |